Mansoura Engineering Journal

Volume 24 | Issue 4 Article 7

12-1-2021

Effect of Operating Conditions on the Mixed Convection in a Channel with Discrete Heat Sources and Partially Filled with Porous Media.

M. El-Kady
Mechanical Power Engineering Department., Faculty of Engineering., El-Mansoura University., Mansoura., Egypt., mselkady@mum.mans.eun.eg

Effect of Operating Conditions on the Mixed Convection in a Channel with Discrete Heat Sources and Partially Filled with Porous Media

تأثير عوامل التشغيل على انتقال الحرارة بالحمل المختلط فى مجرى به منابع حرارية وملء جزئيا بالاوساط المسامية

M. S. El-Kady
Mechanical Power Engineering Department
Mansoura University, Egypt

خلاصـــــــــــــــة

نتيجة التصغير المستمر فى الدوائر الالكترونية، اصبح التصميم الحرارى لهذه الاجهزة بالغ الاهمية، وحيث ان الهدف الرئيسى للتصميم الحرارى هو التبريد والتحكم فى فعالية الجهاز وادرته على العمل فان درجات حرارة المصادر الحرارية حيث امكانية حدوث الانهيار يجب أن تحدد.

يقدم هذا البحث دراسة عمليه لانتقال الحرارة بالحمل المختلط فى مجرى به منبعين حراريين افقيا فى أسفله وملء الفراغ أعلى المنابع بوسط مسامى من شرائح الالمنيوم المسامية، والهدف الرئيسى من الدراسة هو ايجاد مدى تأثير التغير فى حالات التشغيل مثل رقم رينولدز ومعدل انبعاث الحرارة من المنابع الحرارية والتغير فى رقم جراشوف على خواص انتقال الحرارة والمتمثلة فى درجات الحرارة الموضعية والقصوى ورقم نوسيلت. استخدم مجرى اختبار بمقطع رأسى ١٢٠×١٢٠مم وبطول ٢٠٠مم به منبعين حراريين افقيين كل بطول ٤٠مم وعرض ١٢٠مم. وقد اقحم مجرى الاختبار فى مجرى هوائى، واستخدمت شرائح مسامية من معدن الالومنيوم بسمك حوالى ٣مم وكثافة قدرها ١٢٢,٨٥ كجم/م^3 برقم دارسى ٨×١٠$^{-٦}$ كوسط مسامى فى الفراغ أعلى المنابع الحرارية. أمكن تغيير سرعة الهواء بالمجرى حتى ٣ م/ث والتى أعطى امكانية تغيير رقم رينولدز الى ٦٠٠٠، كما تم تغيير معدل انبعاث الحرارة من المنبعيين الحراريين حتى ٧٠١٧ وات/م^2 والذى مكن من تغيير رقم جراشوف حتى ٥٨×١٠^6 . بينت النتائج أن بزيادة رقم رينولدز تتناقص كل من درجتى الحرارة الموضعية والقصوى ويزداد كل من معدل انتقال الحرارة ورقم نوسيلت الموضعى والمتوسط لكل من المنبعيين الحراريين، وانه فى مدى رقم رينولدز أعلى من ٣٤٠٣ يكون معدل التقسان فى كل من درجتى الحرارة الموضعية والقصوى ومعدل الزيادة فى معدل انتقال الحرارة مع الزيادة فى رقم رينولدز قليل جدا بالمقارنة مع نفس التغير فى مدى رقم رينولدز اقل من ٣٤٠٤. ولذا اذا كانت درجة الحرارة القصوى للمنابع الحرارية عند رقم رينولدز= ٣٤٠٤ فى الحدود المسموح بها فى التشغيل فلا يوجد داع لزيادة رقم رينولدز عن ٣٤٠٤ والذى يناظر سرعة هواء تعادل ١,٧م/ث والذى يؤدى الى التوفير فى طاقة التبريد. كما بينت النتائج انه بزيادة رقم جراشوف تتزايد كل من درجات الحرارة الموضعية ومعدل انتقال الحرارة ورقم نوسيلت الموضعى، كما تتزايد درجات الحرارة القصوى للمنابع الحرارية خطيا ويتزايد رقم نوسيلت المتوسط أسيا. واعطت الدراسة علاقات لا بعدية لكل من درجتى الحرارة القصوى ورقم نوسيلت المتوسط للمنبعين الحراريين مع التغير فى كل من رقم رينولدز ورقم جراشوف.

ABSTRACT

An experimental study of laminar mixed convection in a partially filled porous channel with two discrete heat sources on the bottom wall was performed. The main object is to show the effect of Reynolds number, the heat flux, and Grashof number on the heat transfer characteristics. A channel of 120x120mm cross section and length of 200mm is fitted in a low turbulence wind channel. The passages above the heat sources are filled with porous layers and the channel is non-porous elsewhere. The air flow velocity was varied up to 3 m/s which gives a variation of Reynolds number up to 6000, heat flux and Grashof number were varied up to 7017 W/m^2 and $58x10^6$ respectively. Aluminum porous filtration screen sheets of 3mm

Accepted December 20 , 1999

thickness, porosity of 0.95, 122.85 kg/m^3 density, 1.28 x10^{-8} m^2 permeability and Darcy number = 8x10^{-6}, were used as porous layers. The results show that with the increase of Reynolds number, the surface and maximum temperature of the heat sources decrease. and both the local and average Nusselt number increase. For Re>3404 the decrease in maximum temperature and the increase of average Nusselt number are relatively small. Therefore, if the maximum temperatures of the heat sources at Re=3404 are within the safe range of operation, there is no need to increase the Reynolds number over Re =3404, which corresponds to air flow velocity of about 1.7 m/s, which cause a decrease in the required cooling power cost. With increasing the heat flux or Grashof number, the temperatures of the heat sources increase, the heat transfer coefficient increases, the maximum temperature increases linearly and the average Nusselt number increases exponentially. Correlations were obtained for the maximum temperatures and average Nusslet number for both heat sources with Reynolds and Grashof numbers.

INTRODUCTION

One of the serious requirements in the design and operation of modern electronic technologies is an efficient thermal control of the system. For instance, the power intensities in the state of-the-art of electronic computers are extremely high. Consequently, without an effective removal of the excessive heat generated within the devices in place, performance of these sensitive electronic devices deteriorates rapidly.

Recently, the porous substrates are used to improve convection heat or mass transfer in channels or ducts in practical applications and in many technological processes in thermal and chemical engineering. As examples, heat exchangers, heat pipes, electronic cooling, filtration, and chemical reactors are mentioned. Indeed, filling the entire channel with a high conductivity solid matrix can significantly enhance the heat or mass transfer rate but at the expense of a considerable increase of the pressure drop.

Extensive survey of the various modes of convective heat transfer and relevant configurations along with the associated heat transfer and other correlations have been made by Incropera [1], Papanicolaou and Jaluria [2], Bejan and Ledezma [3] and El Kady [4]. Large number of practical situations involve mixed convective heat transfer in which both modes of forced and natural convection effects are dominant. Such circumstances arise when a fluid flows over a heated surface with relatively low velocity. Complete review for the mixed convection in the cooling of protruding heat sources of electronic components have been presented by El Kady [5].

As recently noted by Huang and Vafia [6], very little work has been done on internal forced convection on porous-fluid composite systems. Forced developed convection in a channel partially filled with a porous medium was studied by Poulikakos and Kazmierczak [7] for a parallel-plate channel and circular pipe, and by Chikh et al. [8] for annuli. For both studies, the Dracy Brinkman model was considered, and analytical solutions were derived for the condition of constant heat flux at the wall. It was found that there exists a critical thickness of the porous layer

at which the Nusselt number reaches a maximum. Hadim [9] studied numerically the forced convection in a porous channel with localized heat sources.

In the above literature, the experimental investigations for the use of porous media in the cooling of channels, which have concentrated discrete heat sources, is not found. Therefore, in the previous work of El Kady [5] experiments were done to show the effect of using porous media in the cooling of the channels with discrete heat sources on the heat transfer characteristics. Three cases were presented; the non-porous channel, the fully porous channel, and the partially porous channel (the passages above the heat sources were filled with porous layers, and non-porous are elsewhere). The results for the partially porous channel indicate that almost the same increase in heat transfer, the same decrease in the temperatures and a significant reduction in pressure drop can be obtained compared with the fully porous channel. It shows also that the partially porous technique appears to be promising for application to electronic cooling. Therefore, the present study is another step in this technique. It presents the effect of varying the operating parameters; mainly Reynolds number, heat flux, and Grashof number on the heat transfer characteristics in the partially porous channel which has concentrated discrete heat sources.

EXPERIMENTAL APPARATUS

Figure 1 shows the test rig, which is constructed for the experimental work. The test section (4) in Fig. 1-a is made of wood of 50mm thickness with 120x120mm square cross section and 200 mm long. Two discrete heat sources (5) are embedded in the bottom wall of the test section, to make the heat source face in the same horizontal inside plane of the bottom wall. Each heat source (5) has dimensions of 40 mm length (L), 2.2mm thickness, and 120 mm spanwise with a fixed source spacing ratio S/L = 1.0. The spaces above the two heat sources are filled with porous layers, and the test section is non-porous elsewhere, as shown in Fig. 1-b.

The test section (4) is inserted, as shown in Fig. 1-a, in a low-turbulence wind channel with 120x120mm square cross section and 1300 mm long (6). A centrifugal blower (10), driven by an electric motor (12) is used to draw the air through the system. The blower discharges to a graduated throttle valve (11) by means of which the air velocity through the apparatus may be regulated. To ensure a fairly uniform flow with negligible turbulence through the test section (4), air is drawn through the apparatus by way of a bell mouth (1) and a fine mesh screen (2) as a setting chamber.

Aluminum filtration porous screen sheets, which are used for the purpose of air filtration in the air conditioning devices, are used to form the porous medium. Each aluminum porous sheet is of 40mm length, 120mm wide, thickness of 3 mm and consists of 3 layers of fine aluminum screens. The porous medium is formed from several layers of the aluminum porous screen sheets, which are fitted horizontally above each other to fill the space above the two heaters.

The permeability of the porous medium K is evaluated experimentally as mentioned in Appendix (1) and is found to be $K = 1.28 \times 10^{-8}\ m^2$. The density of the porous sheets was determined experimentally by measuring the mass and volume of the used porous sheets. It took the value of 122.85 kg/m^3. The porosity is calculated as [1.0 – (density of the porous sheets/density of the aluminum metal)]. The porosity was also checked by putting the used aluminum porous sheets in a bottle, which has

the same dimensions of the porous block, and the bottle was then filled with water. The porosity was calculated as the ratio of the water volume to the total volume of the bottle. The porosity took the value of 0.95.

The heat source face is made, as shown in Fig. 1-d, of polished stainless steel sheet (19) with 0.2 mm thickness to prevent the conduction through the heat source surface in the x and z directions. The stainless steel sheet was heated electrically by an electric heater. Two equal lengths of nickel-chromium wire (18) were used as electric heaters for the heat sources. The wire was wound around a mica sheet (17) of 0.5mm thickness and then was sandwiched between other two-mica sheets (17). An auto-transformer (15) is used to control the heat input to the heat sources as well as one voltmeter (13) and an ammeter (14).

The test section is instrumented by 42 copper-constantan thermocouples. The surface temperatures of each heater were measured by 13 copper-constantan thermocouples; nine of them are arranged in the section $z = 0$ and the other four thermocouples are distributed at $z = \pm 3$ cm to ensure the spanwise uniformity. The surface temperatures of the unheated sections were measured by 11 thermocouples of the same kind. The thermocouple distribution along the heater surfaces and the base plate is shown in Fig. 1-c. The upper channel surface temperature was measured by means of 4 thermocouples. The entire junction beads (about 0.25 mm in diameter) of the thermocouples are carefully embedded into the wall, and then grounded flat to ensure that they are flush with the surfaces. The temperature signals are then transferred to a data acquisition unit (Yokogawa) of a sensitivity of 0.1°C (16).

The air velocity is measured with the help of a Pitot tube (3) and an inclined alcohol manometer at the centers of eleven imaginary equal areas into which the Pitot tube is situated and then integrated numerically to obtain the mean air flow velocity. The air velocity is also measured by a hot wire probe (7). The difference in velocity values measured by the two methods is less than ± 1.5%.

The pressure drop across the test section is measured by means of an inclined water manometer.

During the course of the experimental work nearly 1.5 hours were needed to reach the steady state condition. This condition was satisfied when there were no change in the temperature reading within a time period of about 15 minutes.

DATA REDUCTION

The rate of convective heat transfer from the heat source Q was determined from the electrical power input to the heat source Q_e using $Q = Q_e - \Delta Q$, where ΔQ is a small correction for conduction and radiation heat losses. The radiative losses are kept low in the non-porous channel case by employing the polished stainless steel sheet as the heater surface. The emmisivity of polished stainless steel is of order 0.17 as mentioned by Incropera and DeWitt [22]. The radiation heat loss was calculated to be less than 2.5 percent of the total electrical power dissipation, using a simple analytical model. In the case of the porous channel, the radiative losses from the porous surfaces (sides) to the channel surfaces tend to be zero because of the very small difference between their temperatures. The conduction heat losses have been minimized by fixing the heat sources to a wood plate of 5cm thickness. The

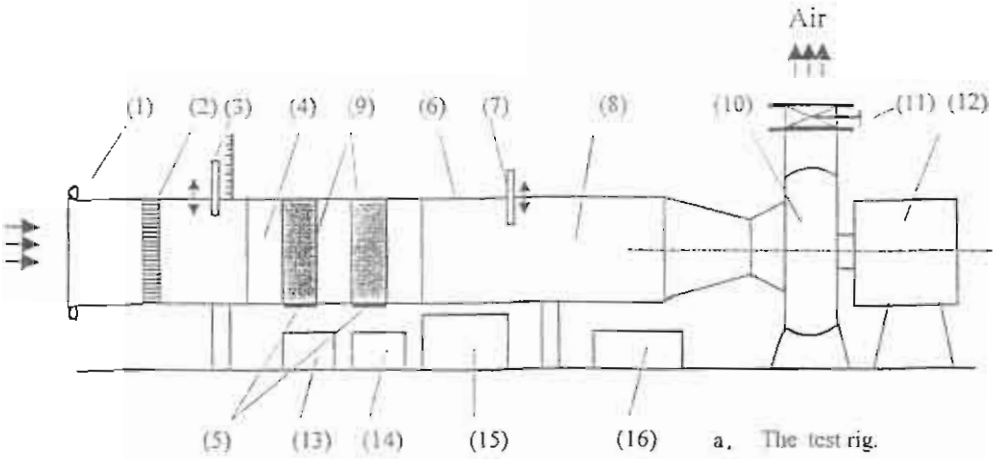

a. The test rig.

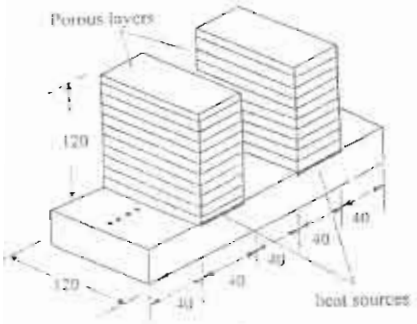

b. Channel base plate with heat sources and porous media

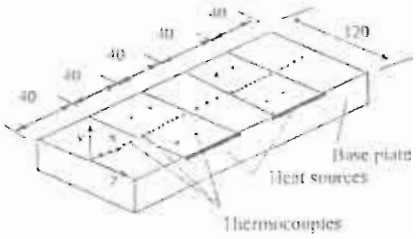

c- Distribution of the thermocouples

Dimensions in mm.

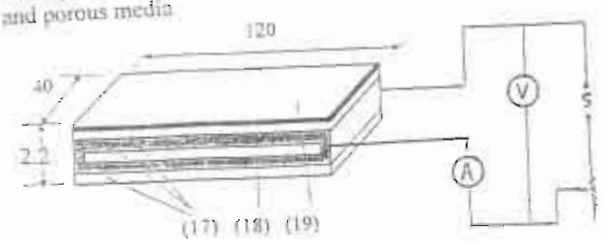

d- Construction of the heat source

Fig. 1 Schematic diagram of test rig

(1) bell mouth, (2) fine mesh screen, (3) pitot tube, (4) test section, (5) heat sources, (6) wind tunnel, (7) hot wire anemometer, (8) transition piece, (9) porous media, (10) blower, (11) blower control valve, (12) electric motor, (13) voltmeter, (14) ammeter, (15) Auto transformer, (16) temperature recorder, (17) mica sheets, (18) nickel-chromium wire, (19) Stainless steel sheet

conduction losses through such surface never exceeds 3.5% by the non-porous case and 2.5% by the porous case of the heat electrical heat input to the heat source.

The average convective heat transfer coefficient $\bar{h}$ for a specific heated section can be defined by:

$$\bar{h} = q / (\bar{T} - T_r) \quad (1)$$

Where q is the convective heat flux and is calculated via q = Q/A where A is the exposed surface area of each heater, $\bar{T}$ is the average temperature of each heated surface and T_r is a reference temperature.

The temperature of the flowing air adjacent to the top surface of the channel was measured by 4 thermocouples as mentioned before. The values of the measured temperatures were always equal to the uniform inlet temperature T_o, which gives that the thermal boundary layer over both heat sources occurs inside the channel. Therefore, the reference temperature T_r can be taken as the uniform inlet temperature T_o. This value is taken also by Hadim [9], Habchi and Acharya [11], Kang et al [12], Kim and Annand [13], Nakayama and Park [14] Young and Wafia [15] and Tso et al. [16] among others.

The local Nusselt number Nu along the surface of the heat source may be expressed in terms of the measured surface heat flux and the surface temperature with respect to the thermal conductivity of the air:

$$Nu = h L/ k = (q. L / k) /(T - T_r) \quad (2)$$

Where T is the local surface temperature

h is the local heat transfer coefficient

k is the air thermal conductivity.

The mean Nusselt number $\bar{Nu}$ for each surface heater is calculated as:

$$\bar{Nu} = (1/A) \int_A Nu.\, dA = (q. L / k) /(\bar{T} - T_o) \quad (3)$$

The other dimensionless parameters which were used in the formulation of the results were Prandtl number Pr, Reynolds number Re, Grashof number Gr, and Darcy number Da, according to the following:

$$Pr = \nu/\alpha, \qquad Re = u_m L/\nu$$

$$Gr = g \beta q L^4/k\nu^2, \qquad Da = K/L^2 \quad (4)$$

Where ν, α, u_m, and β are the air kinematic viscosity, thermal diffusivity, flow mean velocity across the channel section, and volumetric coefficient of thermal expansion, respectively.

RESULTS AND DISCUSSION

Experiments were done of the mixed convection air flow in the channel partially filled with porous medium and has two discrete heat sources in the bottom wall. The main object is to show the effect of the operating parameters such as Reynolds number and Grashof number on the heat transfer characteristics.

Therefore, the passage above the heat sources are filled with porous layers and non-porous elsewhere. The mean air flow velocity was varied up to 3 m/s which gives a variation of Reynolds number up to 6000. heat flux q was varied up to 7017 W/m^2 and Grashof number was varied up to $60x10^6$. The Darcy number of the porous material was calculated to be $8x10^{-6}$, while the geometric parameters were fixed , and took the values of S/L =1, H/L =3.

Effect of Reynolds number

To show the effect of Reynolds number on the heat transfer characteristics, experiments were done for a nearly constant values of heat flux q = 5330 W/m^2 and Gr = $45x10^6$ and the Reynolds number was varied and took fixed values of Re = 1702, 2127, 3404, 3723, and 5531. Figure 2 presents the variation of surface temperature difference ($T-T_o$) of the heat sources surfaces. The surface temperature is characterized by nearly ambient temperature until the leading edge of the first heat source, sharp rise in the surface heat source temperature due to heat input, and followed by gradual decay downstream. The temperature of the heat sources surface decreases with the increase of Reynolds number. This fact is shown also in table 1, which presents the temperatures of the leading and trailing edges and the difference between them for both the first and second heat sources for the different values of Reynolds number. Both Fig. 2 and table 1 show that the difference in temperature between the trailing and leading edges of each heater are nearly constant. It is nearly 13.4°C and 16.8°C with a change of nearly ± 4.5 percent for the first and second heat sources respectively. Also the temperature levels along the second heat source are higher than those of the first heat source due to the hotter air flowing over the second heat source.

Figure 3 shows the variation of the dimensionless maximum temperature θ_{max}, where $\theta = [(T-T_o)/T_o]$ of each heat source with the variation of Reynolds number, at q=5330 W/m^2 and Gr = $45x10^6$. The dimensionless maximum temperature decreases with increasing Reynolds number. The decrease of the maximum temperature is only 0.168 and 0.192 for the first and second heaters with increasing Reynolds number from 3404 to 5531 respectively. Mainly, increasing Reynolds number with about 60 percent decreases the maximum temperatures with about 9 and 7 percent for the first and second heat sources respectively. This indicates that there is no need to increase the Reynolds number above Re =3404, which corresponds to airflow velocity of about 1.7 m/s.

Figure 4 represents the variation of heat transfer coefficient along the heat sources with the variation of Reynolds number, at q = 5330 W/m^2 and Gr =$45x10^6$. Table 1 shows also the heat transfer coefficient for both heat sources. Both Fig. 4 and Table 1 present that the heat transfer coefficient increases with increasing Reynolds number. They show also that the heat transfer coefficient increases from 144.3 to 158.4 by about 10 percent for the first heat source and from105.6 to 113.8 by about 8 percent for the second heat source with increasing Reynolds number from 3404 to 5531 respectively. This relatively small increase presents that if the maximum temperatures of the heat sources at Re=3404 are within the safe range of operation, there is no need to increase the Reynolds number above Re =3404 which corresponds to mean air flow velocity of about 1.7 m/s.

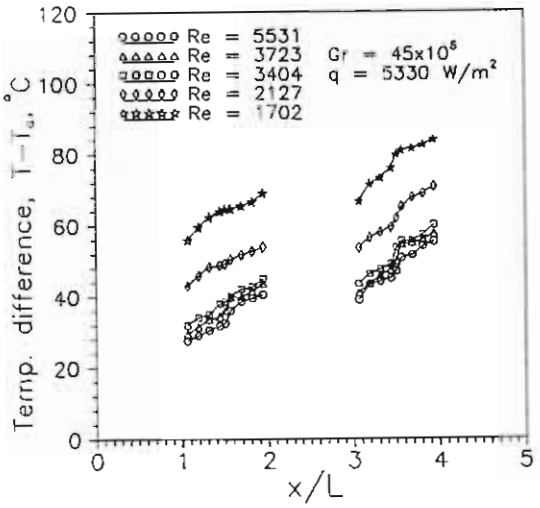

Fig. 2 Variation of surface temperature ($T-T_o$) of the horizontal base plate of the channel with the variation of Reynolds number at q = 5330 W/m^2 and Gr =45x10^6

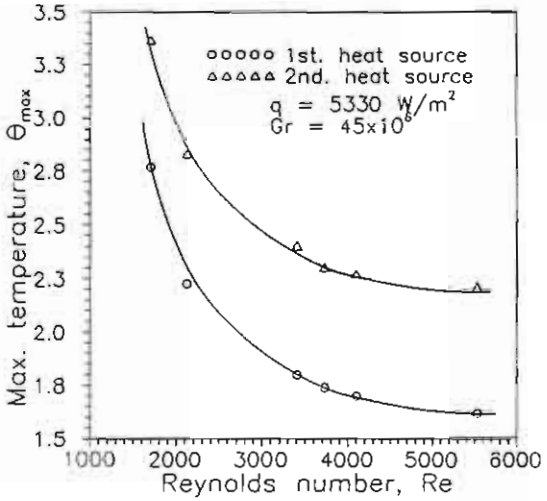

Fig. 3 Variation of the dimensionless maximum temperature of each heat source with the variation of Reynolds number, at q = 5330 W/m^2 and Gr = 45x10^6

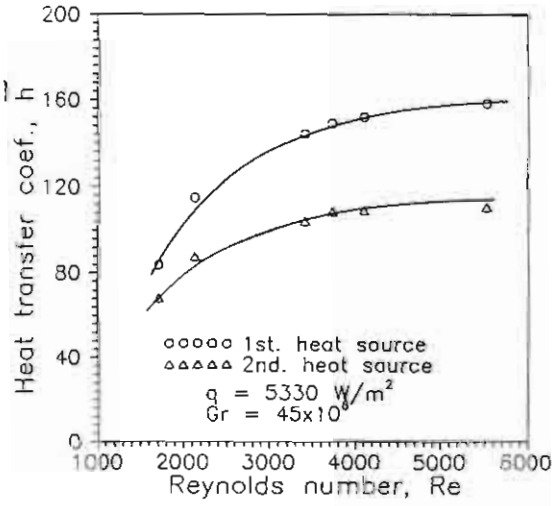

Fig. 4 Variation of heat transfer coefficient along the heat sources with the variation of Reynolds number, at q = 5330 W/m^2 and Gr = 45x10^6.

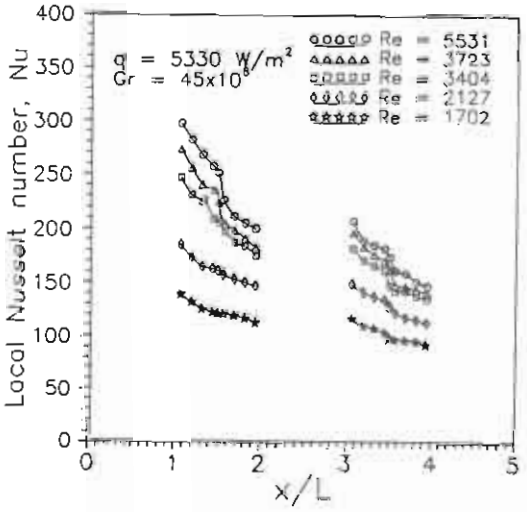

Fig. 5 Effect of Reynolds number on the local Nusselt number along the heat sources at q = 5330 W/m^2 and Gr =45x10^6

The variation of the local Nusselt number along the surfaces of the first and second heat sources with the variation of Reynolds number is presented in Fig.5. Above each heat source the local Nusselt number begins with its maximum value at the leading edge, then it decreases with the increase of the distance from the leading edge, and the minimum value occurs at the trailing edge. Also the increase of Reynolds number increases the local Nusselt number. Table 2 presents the local Nusselt number of the leading and trailing edges and the difference between them for both the first and second heat sources. Both Fig. 5 and Table 2 show that the difference in local Nusselt number between the trailing and leading edges along the heat source, increase with the increase of Reynolds number. Also the local Nusselt number levels along the second heat source are smaller than those of the first heat source due to the hotter air flowing over the second heat source.

Table 1: The temperatures ($T-T_o$) of the leading and trailing edges and coefficient of heat transfer for both heat sources at $q=5530$ W/m^2 and $Gr = 45x10^6$

Re	first heat source				Second heat source			
	$T - T_o$			h	$T - T_o$			h
	leading edge	Trailing edge	differ-ence		Leading edge	Trailing edge	differ-ence	
1702	55.8	69.2	13.4	82.1	66.7	84.2	17.5	67.8
2127	39.9	52.7	12.8	114	51.5	68.8	17.1	87
3404	31.9	45	13.1	144.3	43.5	60.1	16.6	105.6
3723	29.5	43.5	14	148.9	41.5	57.6	16.1	108.4
5531	27.6	40.8	13.2	158.4	39.1	55.3	17.2	113.8

Table 2: Local Nusselt number of the leading and trailing edges, and average Nusselt number for both heat sources at $q = 5530$ W/m^2 and $Gr = 45x10^6$

Re	First heat source				Second heat source			
	Nu			$\bar{Nu}$	Nu			$\bar{Nu}$
	leading edge	Trailing edge	differ-ence		Leading edge	Trailing edge	differ-ence	
1702	140.51	114.7	25.8	124.8	118.8	94.34	24.46	103
2127	186.75	148.6	38.15	173.3	150.8	113	37.8	132.2
3404	248.4	176.1	72.3	219.3	182.2	136.9	45.3	160.5
3723	274.38	183.8	90.58	226.3	197.43	141.76	55.67	164.8
5531	298.48	202	96.48	240.8	207	148	59	173.4

Figure 6 represents the variation of average Nusselt number along the heat sources with the variation of Reynolds number, for $q = 5330$ W/m^2 and $Gr = 45x10^6$. Table 2 shows also the average Nusselt number for both heat sources. Both Fig. 6 and Table 2 present that the average Nusselt number increases with the increase of Reynolds number. With the increase of Reynolds number from 3404 to 5531, the average Nusselt number increases from 219.3 to 240.8 by about 10 percent for the first heat source and from 160.5 to 173.4 by about 8 percent for the second heat source, respectively. This relatively small increase presents that if the maximum temperatures of the heat sources at Re=3404 are within the safe range of the operation, there is no need to increase the Reynolds number above Re =3404 which corresponds to air flow velocity of about 1.7 m/s

Effect of Grashof number

To show the effect of Grashof number on the heat transfer characteristics, experiments were done for a nearly constant values of Re = 1702, 2127, 3404, 3723 and 5531 and the heat flux was increased up to 7017W/m^2 with an increase of Grashof number up to Gr = 58.05×10^6. Figure 7 presents the surface temperature difference ($T-T_o$) of the heat sources. The surface temperature of both the heat sources decreases with the decrease of the heat flux. This fact is shown also in table 3, which presents the temperatures of the leading and trailing edges and the difference between them for both the first and second heat sources at the different values of Grashof number. Both Fig. 7 and table 3 show that the temperature difference between the trailing and leading edges of the heat sources increases with increasing heat flux or Grashof number. Also, in spite of the temperature levels along the second heat source are higher than those of the first heat source, the temperature differences between the leading and trailing edges of the second heat source are smaller than those of the first heat source.

Figure 8 shows the variation of the dimensionless maximum temperature of each heat source with the variation of Grashof number, at Re = 1702, 2127, 3404, 3723 and 5531. The maximum temperature increases linearly with the increase of Grashof number or the heat flux

Table 3: The temperatures ($T - T_o$) of the leading and trailing edges and coefficient of heat transfer for both heat sources at Re=3723

.q	$Grx10^{-6}$	first heat source			.h	Second heat source			.h
		$T - T_o$				$T - T_o$			
		leading edge	trailing edge	differ-ence		Leading edge	trailing edge	differ-ence	
104	0.936	0.2	1.4	1.2	140	1.2	1.5	0.3	80.23
406	3.63	2	3.6	1.6	146.7	3.4	4.7	1.3	86.7
906	8.05	2.8	8.1	5.3	150	7.6	10.8	3.2	96.6
1625	14.32	4.3	13.8	9.5	153.5	13.1	17.6	4.5	99.8
2604	22.25	6.5	20.7	14.2	158	18.5	28	9.5	102.5
4069	37.665	18.6	34.7	16.1	163	31.8	46.2	14.4	105
5330	44.96	29.5	48.5	19	164.3	42	57.6	16.6	107.3
7017	58.054	35.2	59.3	24.1	165	53.3	75.2	21.9	108.5

Figure 9 represents the variation of heat transfer coefficient along the heat sources with the variation of Reynolds number, for Re=3723. Table 3 shows also the heat transfer coefficient for both heat sources. Both Fig. 9 and Table 3 present that the heat transfer coefficient increases with the increase of Grashof number or the heat flux.

Figure 10 represents the variation of average Nusselt number along the heat sources with the variation of Grashof number, at Re = 1702, 2127, 3404, 3723 and 5531. With the increase of Grashof number, the average Nusselt number increases exponentially.

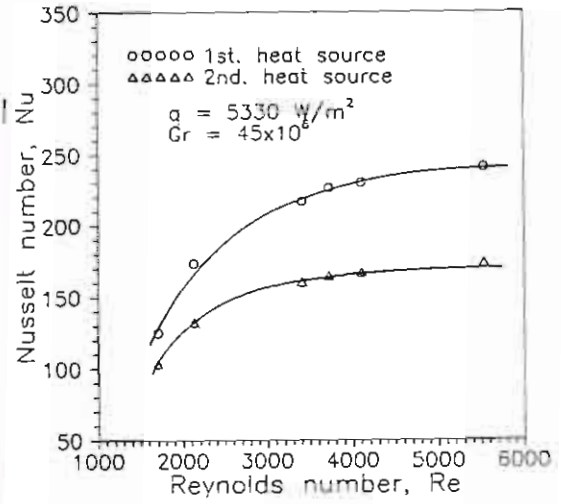

Fig. 6 Effect of Reynolds number on the average Nusselt number along the heat sources at q = 5330 W/m^2 and Gr =45x10^6

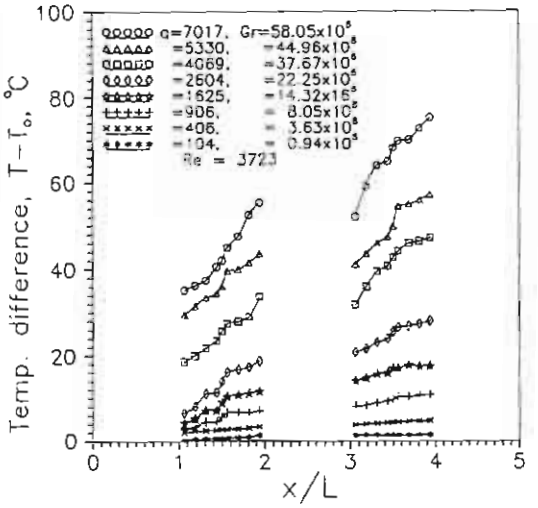

Fig. 7 Variation of surface temperature (T-T$_\infty$) of the horizontal base plate of the channel with the variation of heat flux, at Re = 3723

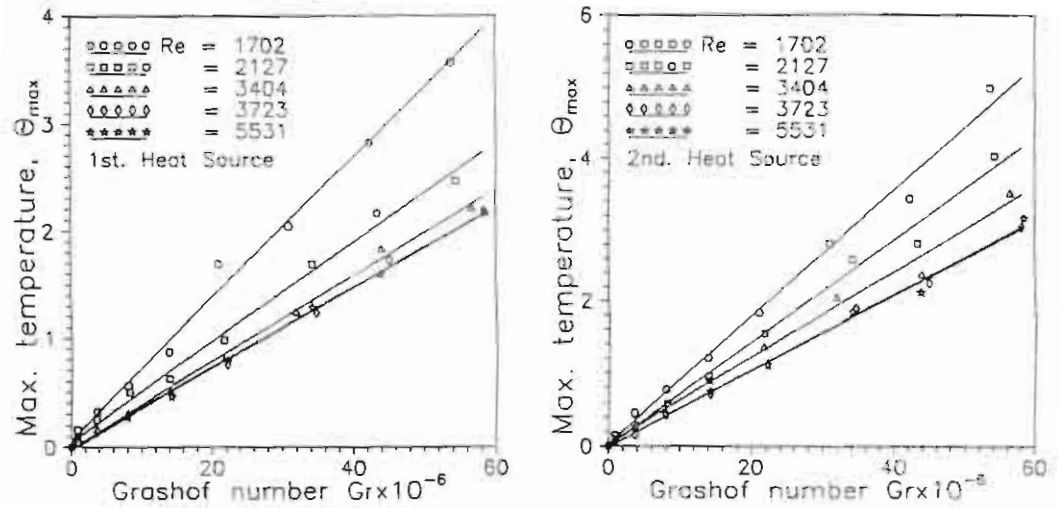

Fig. 8 Effect of the Grashof number on the dimensionless maximum temperature of each heat source

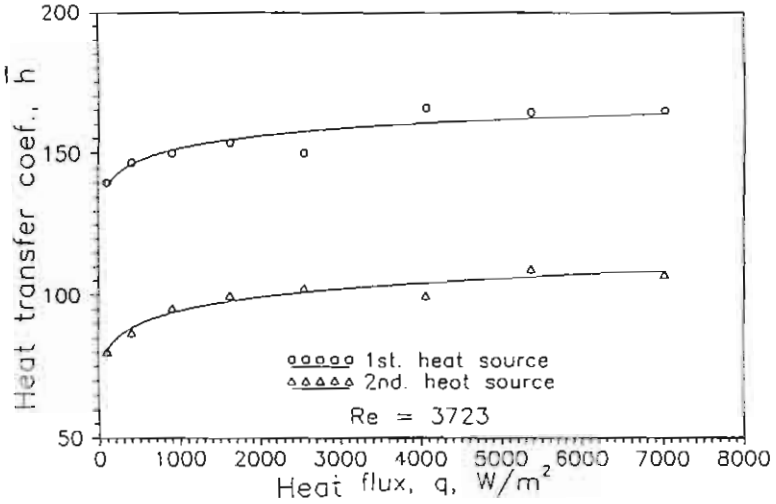

Fig. 9 Effect of the heat flux on the heat transfer coefficient $\bar{h}$ along the heat sources, at Re=3723

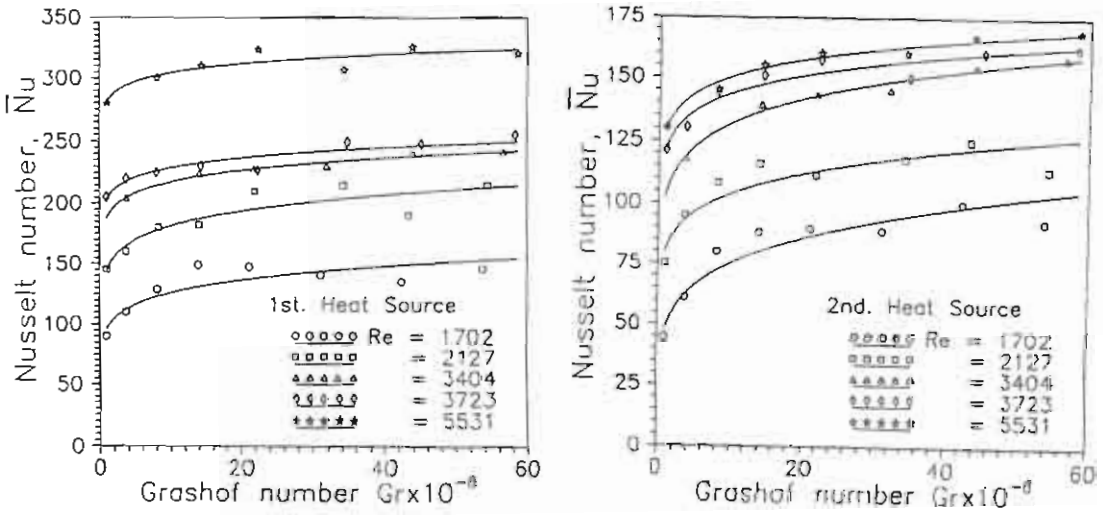

Fig. 10 Variation of average Nusselt number $\bar{Nu}$ along the heat sources with the variation of Grashof number

Correlations

The variation of the maximum temperature for the first and second heat sources with the variation of both Reynolds and Grashof numbers can be correlated for the range of $Gr \leq 58.05 \times 10^6$ and $1702 \leq Re \leq 5531$ due to Fig. 8 as follows:

$$\theta_{max1} = [102.6 - 29.8 \times 10^{-3} Re + 3.3 \times 10^{-6} Re^2] \times 10^{-9} Gr$$
$$\theta_{max2} = [134 - 35.2 \times 10^{-3} Re + 3.6 \times 10^{-6} Re^2] \times 10^{-9} Gr \quad (5)$$

Where θ_{max1} and θ_{max2} are the dimensionless maximum temperatures of the first and second heat sources respectively.

The variation of the Nusselt numbers for the first and second heat sources with the variation of both Reynolds and Grashof numbers can be correlated for the range of $Gr \leq 58.05 \times 10^6$ and $1702 \leq Re \leq 5531$ due to Fig. 10 as follows:

$$\bar{Nu}_1 = [-50.1 + 40.6 \times 10^{-3} Re] . Gr^{[0.1455 - 2.2 \times 10^{-5} Re]}$$
$$\bar{Nu}_2 = [-12.23 + 12.4 \times 10^{-3} Re] . Gr^{[0.197 - 2.7 \times 10^{-5} Re]} \quad (6)$$

CONCLUSIONS

Experiments were done on the mixed convection airflow in the channel partially filled with porous medium (the passage over the heat sources are filled with porous layers with Darcy number = 8×10^{-6}, and is non-porous elsewhere), and has two discrete heat sources in the bottom wall. The effect of Reynolds number and Grashof number on the heat transfer characteristics was tested. Reynolds number was varied up to 6000, heat flux was varied up to 7017 W/m^2 and Grashof number was varied up to 60×10^6. The following conclusions can be considered:

The temperature levels along the second heat source are higher than those of the first heat source. While, the local Nusselt number levels along the second heat source are smaller than those of the first heat source due to the hotter air flow over the second heat source.

With increasing Reynolds number, the maximum temperatures of both the heat sources decrease, and both the local and average Nusselt number increase. For Re>3404 the decrease in maximum temperature and the increase of average Nusselt number are relatively small. Therefore, if the maximum temperatures of the heat sources at Re=3404 are within the safe range of operation, there is no need to increase Reynolds number above Re = 3404 which corresponds to air flow velocity = 1.7 m/s, which cause a decrease in the required cooling power cost.

With increasing the heat flux or Grashof number, the temperature of the heat sources, the temperature difference along them and the heat transfer coefficient increase, the maximum temperature increases linearly and the average Nusselt number increases exponentially.

The dimensionless temperatures and the average Nusselt numbers along the two heat sources were correlated with Reynolds number and Grashof number.

NOMENCLATURE

A	Surface area of each heat source, m^2
Da	Darcy number, $Da = K/L^2$
Gr	Grashof number, $Gr = g\beta L^4 q / k\upsilon^2$
h	Convective heat transfer coefficient, $W/m^2.K$
H	Channel height, m
k	Fluid thermal conductivity, W/m K
K	Permeability of the porous media, m^2
L	Heater width, m
Nu	Local Nusselt number
$\overline{Nu}$	Average Nusselt number
Pr	Fluid Prandtl number, υ/α
q	Heat flux on the heat source surface, W/m^2
Q	Power input to each heat source, W
Re	Fluid Reynolds number, $Re = u_m L/\upsilon$
S	Distance between the heat sources, m
T	Fluid temperature, C,
T_o	Uniform air temperature at channel entrance, C
u_m	Air mean velocity at channel entrance, m/s
x	Distance in horizontal direction, m
y	Distance in vertical direction, m
z	Distance in normal direction, m
α	Fluid thermal diffusivity, m^2/s
β	Fluid volumetric coefficient of thermal expansion, 1/K
θ	Dimensionless temperature
υ	Fluid kinematic viscosity, m^2/s

REFERENCES

1. Incropera, F., P., "Convection Heat Transfer in Electronic Equipment Cooling," ASME J. of Heat Transfer, Vol. 110, pp. 1097-1111, 1988.
2. Papanicolaou, E., and Jaluria, Y., "Mixed Convection From Simulated Electronic Components at Varying Relative Positions in a Cavity," ASME J. of Heat Transfer, Vol. 116, pp. 960-970, 1994.
3. Bejan, A, and Ledezma, G. A., "Thermodynamic optimization of cooling techniques for Electronic Packages," I. J. Heat Mass Transfer, Vol. 39, pp. 1213-1221, 1996.
4. El Kady, M. S., "Natural Convection From Dual Surface Heat Sources in a Vertical Rectangular Enclosure," Mansoura Engineering Journal (MEJ), Vol. 23, No. 3, pp.M.41-M.55, September 1998.
5. El Kady, M. S., "Enhancement of Mixed Convection in a Channel with Discrete Heat Sources by Using Porous Media," To be published

6. Huang, P.C., and Vafia, K., "Analysis of Flow and Heat Transfer Over an External Boundary Covered with a Porous Substrate" ASME Heat Transfer, Vol.116, pp. 768-771, 1994.
7. Poulikakos, D., and Kazmierczak, M., "Forced Convection in a Duct Partially Filled with a Porous Material," Journal of Heat Transfer, Vol. 109, pp. 653-662, 1987.
8. Chikh, A., Boumedien, A, Bouhadef, K, and Lauriat, G., "Non-Darcian Forced Convection Analysis in an Annulus Partially Filled with a Porous Material," Numerical Heat Transfer, Part A, Vol. 28, pp. 707-722, 1995.
9. Hadim, A., "Forced Convection in a Porous Channel with Localized Heat Sources," ASME Journal of Heat Transfer, Vol. 116, pp. 465-472, 1994.
10. Incropera, F. P., and DeWitt, D. P., "Introduction to Heat Transfer," John Willey & Sons, Third Edition, pp. 767, 1996.
11. Habchi, S., and Acharya, S., "Laminar Mixed Convection in a Partially Blocked, Vertical Channel," Int. J. Heat Mass Transfer, Vol. 29, pp. 1711-1722, 1986
12. Kang, B. H., Jaluria, Y., and Tewari, S. S., "Mixed Convection Transport From an Isolated Heat Source Module on a Horizontal Plate," ASME J. of Heat Transfer, Vol. 112, pp. 653-661, 1990.
13. Kim, S., and Anand, N., "Laminar Developing Flow and Heat Transfer between a Series of Parallel Plated with Surface Mounted Discrete Heat Sources," I. J. Heat Mass Transfer, Vol. 37, No. 15, pp. 2231-2244, 1994.
14. Nakayama, W., and Park, S. H., "Conjugate Heat Transfer from a Single Surface-Mounted Block to Forced Convective Air Flow in a Channel," ASME Journal of Heat Transfer, vol.118 pp301-309, 1996.
15. Young, T.J., and Vafia, K., "Experimental and Numerical Investigation of Forced Convective Characteristics of Arrays of Channel Mounted Obstacles," ASME Journal of Heat Transfer, Vol. 121, pp. 34-42, 1999.
16. Tso, C. P., Xu, G. P., and Tou, K. W.,"An Experimental Study on Forced Convection Heat Transfer From Flush-Mounted Discrete Heat Sources." ASME Journal of Heat Transfer, Vol. 121, pp. 326-332, 1999.

APPENDIX 1: CALCULATION OF THE PERMEABILITY

Henry Darcy observed that the volume rate of flow through any pipe packed with porous medium was proportional to the negative of the pressure gradient. This relationship, known as Darcy's law, after being modified to include the fluid viscosity, can be stated as follows:

$$\partial P/\partial x = -\mu u_m/K$$

Where μ is the dynamic viscosity of the fluid seeping through the porous material and $\partial P/\partial x$ represents the pressure gradient in the direction of flow.

From this theory the permeability K can be determined as follows:

$$K = -\mu u_m/(\partial P/\partial x)$$

Experiments were done for the airflow through the fully filled porous channel. Both the air velocity and the pressure drop were measured. The relation between the pressure gradient (VP/Vx) and the term (μu_m) was drawn and the permeability was then determine as the negative of the slope of the line which gives $K=1.28 \times 10^{-8}$ m^2